Clays and Clay Minerals, Vol. 59, No. 1, 34–41, 2011.

REMOVAL OF RUTHENIUM FROM AQUEOUS SOLUTION BY CLINOPTILOLITE

MAHBOOBEH KABIRI-TADI[1] AND HOSSEIN FAGHIHIAN[2,*]

[1] Department of Chemistry, University of Isfahan, 81746-73441, Isfahan, Iran
[2] Department of Chemistry, Islamic Azad University, Shahreza Branch, Iran

Abstract—Ruthenium compounds are highly toxic and carcinogenic. In the present study, clinoptilolite was used in the removal of Ru species from aqueous solutions. Clinoptilolite is a good choice of sorbents because it is naturally abundant and therefore cheap. After the process where Ru was removed from the aqueous solution, the clinoptilolite was characterized by X-ray diffraction, X-ray fluorescence, thermogravimetric analysis, and Fourier-transform infrared spectroscopy techniques. The influence of pH, contact time, and temperature on the adsorption of Ru was investigated and the optimum conditions were found to be 2 h of contact time and pH = 2. Pseudo first-order, pseudo second-order, Elovich, and intra-particle diffusion models were used to analyze the adsorption-rate data. The pseudo second-order model was found to be the best kinetics model in terms of matching the experimental results obtained. Adsorption isotherms were constructed to assess the maximum adsorption capacity of clinoptilolite. The Langmuir model fitted the data reasonably well in terms of regression coefficients. Adsorption studies were also performed at different temperatures to calculate the thermodynamic parameters. The numerical value of ΔG^0 decreased with increasing temperature, indicating that adsorption is favored at higher temperatures. The positive values of ΔH^0 corresponded to the endothermic nature of the adsorption processes. The proposed method of removal is applicable at an industrial scale.

Key Words—Adsorption, Aqueous Solution, Clinoptilolite, Removal, Ruthenium.

INTRODUCTION

Ruthenium is a rare element found in ~10^{-8}% of the Earth's crust and usually occurs in association with other platinum group metals. Ruthenium and its compounds are used for many industrial purposes, *e.g.* alloys with other metals in the manufacture of electrical wires, electrodes, incandescent-bulb filaments, and laboratory equipment. Ruthenium and its compounds also catalyze chemical processes. They are also used in the chemical industry, in electroplating, in electrocoating, and as redox indicators (Avtokratova, 1963). Ruthenium is widely used in the electronics industry and as one of the most effective hardeners in high-density alloys. Platinum metals, especially Ru and its chlorocomplexes, have been used widely in the catalytic oxidation of some organic compounds (Rard, 1985). The hazards associated with all Ru compounds are that they are highly toxic and carcinogenic, and they stain the skin severely.

Separation procedures including volatilization, coprecipitation, solvent extraction, sorption, and chromatography can be used to isolate and preconcentrate Ru from multicomponent samples containing noble and base metals (Balcerzak, 2002; Hong and Grubbs, 2007; Lopez *et al*., 2009; Knight *et al*., 2010; Kokate and Kuchekar, 2010). Separation of Ru has also been achieved by coprecipitation, sequential distillation, precipitation, and adsorption onto inorganic materials (Gandon *et al*., 1993; Granados *et al*., 2004; Rathore *et al*., 2004; El-Absy *et al*., 2005). Other methods used in the removal of metal ions from solutions include chemical precipitation, ultra-filtration, biochemical treatment, ion exchange, and adsorption (Nassar *et al*., 2004). The adsorption of pollutants from solution plays an important role in waste-water treatment as it eliminates the need for huge sludge-handling processes. Adsorption is preferred over other processes because it is cheaper and because of the effluents it produces – well designed sorption processes are more efficient and result in effluents which can be recycled or disposed of more safely. Gallium arsenide, Fe oxides, activated charcoal, and zeolites have been used in the adsorption of Ru (Musić and Ristic, 1987; Schlesinger *et al*., 1990; Dyer and Aggarwal, 1995; Qadeer, 2007).

Zeolite-containing rocks are used in waste-water purification to remove toxic and radioactive elements (Breck, 1974). Zeolites are thermally stable, resistant to radiation, and are widely available throughout the world. They are used frequently in sorption processes because of their low cost and ion selectivity (Arambula-Villazana *et al*., 2006; El-Naggar *et al*., 2008). Clinoptilolite is a natural zeolite that has been considered for radioactive-waste treatment (Elizondo *et al*., 2000; Osmanlioglu, 2006; Borai *et al*., 2009; Sharma *et al*., 2009). Clinoptilolite belongs to the most widely available family of zeolites. The ideal composition is $Na_6[Al_6Si_{30}O_{72}].24H_2O$ (Barrer, 1985). Reserves of clinoptilolite-rich tuffs have been found throughout the world (Schüth *et al*., 2002).

* E-mail address of corresponding author:
Faghihian@iaush.ac.ir
DOI: 10.1346/CCMN.2011.0590106

The aim of this work was to study the efficiency of natural clinoptilolite in the adsorption of Ru species from aqueous solutions. The effects of different parameters such as initial concentration, initial pH of the solution, and temperature on the adsorption process were studied.

Experimental

Reagents and methods

All chemical reagents (obtained from Merck, Darmstadt, Germany) used in this study were of analytical reagent (AR) grade and were used without further purification. All solutions were prepared in double distilled water. Ruthenium ions were obtained as Ru trichloride hydrate (also from Merck, Darmstadt, Germany).

Natural clinoptilolite was obtained from deposits in Semnan, Iran; the zeolite was crushed and pulverized in a mortar and sieved to a particle size of 100−224 μm. The powder was refluxed in distilled water in order to remove soluble salts and then washed and dried at 110ºC. The powder was stored in a desiccator over saturated NaCl solution in order to maintain a constant vapor pressure throughout the period of the experiments. The purified sample was characterized by X-ray diffraction (XRD), Fourier-transform infrared (FTIR) spectroscopy, and thermal analysis. The XRD patterns were collected using a Bruker, D8 ADVANCE X-ray diffractometer with CuKα radiation (wavelength: 1.5406 Å; Ni filter) up to 45º2θ at ambient temperature. The Na, K, Ca, Si, and Al contents of the sample were determined using a Bruker, S4 PIONEER X-ray fluorescence spectrometer. The FTIR spectrum of the clinoptilolite was obtained using a Nicolet Impact 400D Model spectrophotometer (Nicolet Impact, Madison, Wisconsin, USA) using the KBr pressed-disk technique. For each KBr pellet, 1 mg of zeolite and 100 mg of KBr were weighed, ground in an agate mortar, and pressed. Spectra were recorded in the wavenumber range 400−4000 cm^{-1}. Thermogravimetric analysis (TGA) was performed using a Mettler, TG-50 thermal analyzer from ambient temperature to 800ºC at a heating rate of 10ºC min^{-1} in air. The determinations of Ru ions were carried out using an inductively coupled plasma-atomic emission spectrometer model Integra-XL (GBC, Adelaide, Australia).

Adsorption experiments

To discover the optimum conditions, the adsorption of Ru was studied by batch technique. A sample of 0.3 g of zeolite was equilibrated with 10 mL of Ru solution of known concentration at fixed temperature for a known period of time. After equilibration, filtration of the solid phase was followed by centrifugation of the filtrate (3000 rpm for 5 min). 5 mL of the supernatant solution was then taken for Ru measurement. The amount of Ru adsorbed was calculated from the difference in concentrations before and after adsorption.

$$q = (C_i - C_f) \times V/m \quad (1)$$

where q is the amount of metal ions adsorbed by a unit mass of zeolite (meq g^{-1}); C_i and C_f are the initial and final Ru concentrations (meq L^{-1}), respectively; m is the amount of zeolite used (g); and V is the volume of Ru solution (L).

The effects of different parameters, including initial Ru concentration, the solution pH, the contact time, and the temperature were investigated.

RESULTS AND DISCUSSION

Physicochemical characterization

X-ray diffraction patterns of the purified clinoptilolite and of a material examined by Treacy and Higgins (2007) were compared (Figure 1). Clinoptilolite was the major phase found in the zeolite-rich rock examined.

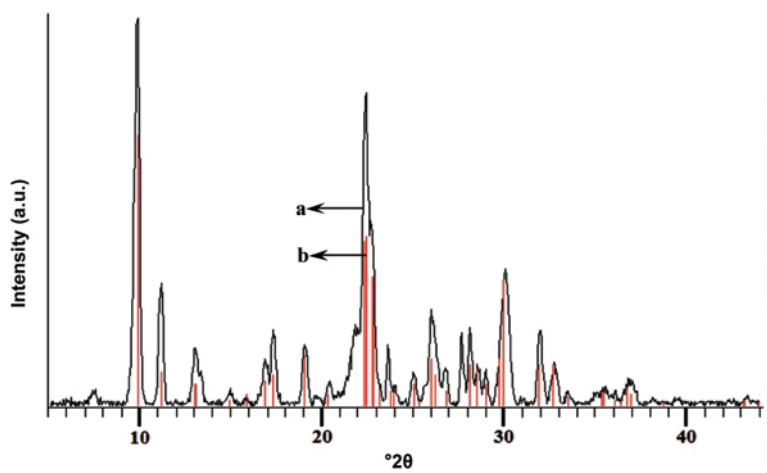

Figure 1. XRD patterns of the natural zeolite (a, black line) and of material examined by Treacy and Higgins (2007) (b).

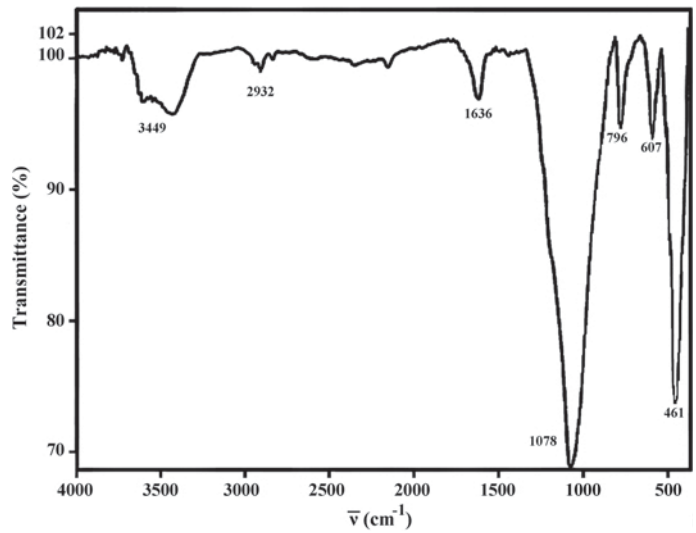

Figure 2. FTIR spectrum of clinoptilolite.

The zeolites were significantly hydrated as illustrated by discrete water absorption bands in their 3500 and 1640 cm^{-1} regions (Figure 2). These bands, which were centered at 3449 and 1636 cm^{-1}, refer to water molecules associated with Na and Ca in the channels and cages of the zeolite structure. Other bands near the 1078 cm^{-1} band, arising from asymmetric stretching vibration modes of internal *T*–O bonds in TO_4 tetrahedra (*T* = Si and Al), were also observed. The 796 and 461 cm^{-1} bands are assigned to the stretching vibration modes of O–*T*–O groups and the bending vibration modes of *T*–O bonds, respectively (Wilson, 1994; Tanaka *et al*., 2003).

The chemical composition of the zeolite was obtained by XRF (Table 1). The Si/Al ratio of the natural clinoptilolite studied was 5.086 which is within the range (4–5.5) suggested by Breck (1974).

Table 1. Chemical composition of purified clinoptilolite obtained by the XRF method.

Species	Wt. (%)
SiO_2	67.71
Al_2O_3	11.30
Na_2O	2.39
CaO	2.09
K_2O	1.86
MgO	0.696
Fe_2O_3	0.439
TiO_2	0.116
SrO	0.107
BaO	0.059
LOI*	13.2
Total	99.97

* Loss on ignition

In the TG and DTG curves of the natural sample (Figure 3), a characteristic dehydration peak between 25 and 200ºC with a 13.1% weight loss was observed.

Optimization of conditions

The adsorption of Ru species was at its greatest at pH 2 (Figure 4) so the present adsorption studies were carried out at that pH.

Electrochemical and spectral studies on $RuCl_3$ in aqueous solution in the pH range 0.4–2.0 have shown that Ru(III) may exist as four major species,

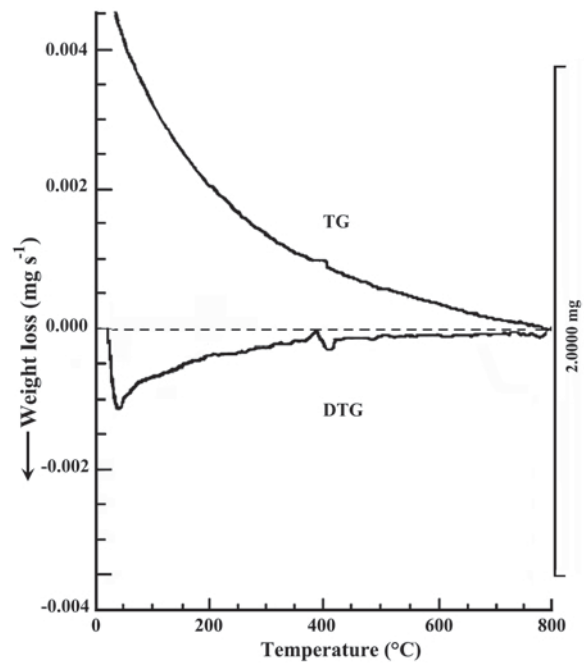

Figure 3. TG and DTG curves of clinoptilolite.

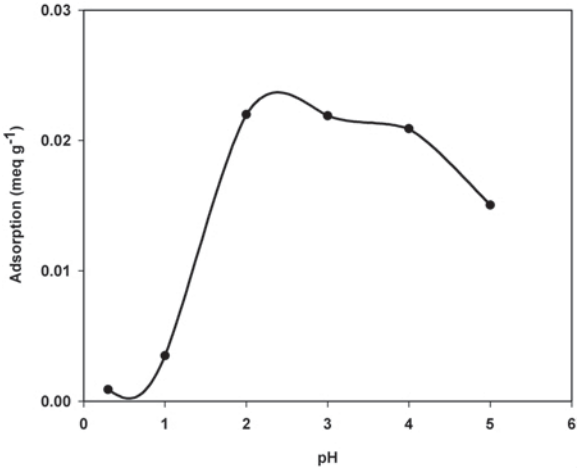

Figure 4. Effect of pH on adsorption of Ru (Ru concentration = 2.5×10^{-4} mol L^{-1}, temperature = 25ºC, and contact time = 1 h).

$[RuC1_4(H_2O)_2]^-$, $[[RuC1_3(H_2O)_3]$, $[RuC1_2(H_2O)_4]^+$, and/or $[RuC1(H_2O)_5]^{2+}$. They are referred to here as species 1, 2, 3, and 4, respectively. The approximate concentrations of these complexes in solution were: at pH 0.40, 1 + 2 = 47.2%, 3 = 31.6%, and 4 = 21%; at pH 1, 1 = 12.1%, 2 = 36.6%, 3 = 40.4%, and 4 = 11%; at pH 2, only species 3 was present (Taqui Khan *et al*., 1986). The charge repulsion between the zeolite surface and negatively charged species of Ru at pH<2.0 may be one of the reasons for poor adsorption at these pH values. Competition with H_3O^+ is another possible reason. At higher pH values, hydroxyl ions are introduced gradually to the coordination sphere and negatively charged Ru complexes are produced.

The results show that as contact time increased, Ru adsorption increased initially, but then approached a constant value rapidly (Figure 5). Equilibrium was attained after 2 h, after which time no further significant increase occurred in the level of adsorption. After just 15 min, 92% of the amount of adsorption at equilibrium had been achieved. A shaking time of 2 h employed for all of the equilibrium adsorption studies was sufficient to ensure that adsorption equilibrium was reached.

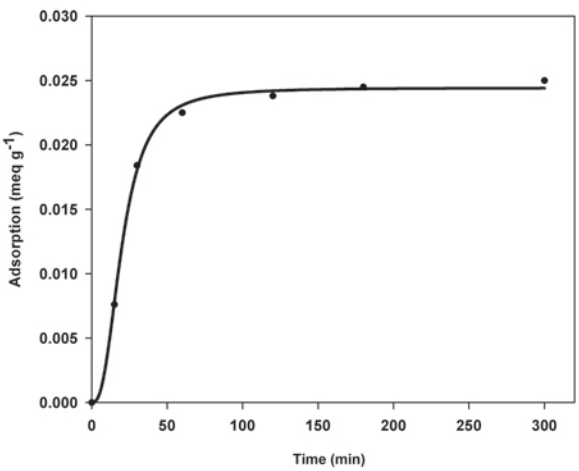

Figure 5. Effect of contact time on adsorption of Ru (Ru concentration = 2.5×10^{-4} mol L^{-1}, temperature = 25ºC, and pH = 2.0).

Adsorption kinetics and thermodynamics

The adsorption kinetics of Ru complexes from the liquid phase was evaluated by applying four different models, namely, pseudo first-order, pseudo second-order, the Elovich equation, and the intra-particle diffusion model. These models were tested to fit the experimental data obtained by batch experiments.

The pseudo first-order equation is generally expressed as follows:

$$\frac{dq}{dt} = K_1(q_e - q_f) \tag{2}$$

where q_e and q_t are the amounts of species adsorbed per unit weight (mmol g^{-1}) of sorbent at equilibrium and at any time t, respectively, and K_1 is the rate constant of pseudo first-order sorption (min^{-1}). After integration and applying the boundary condition of $q = 0$ at $t = 0$, the integrated form of the equation becomes:

$$\ln(q_e - q_t) = \ln q_e - K_1 t \tag{3}$$

The pseudo second-order equation (Blanchard *et al*., 1984) based on adsorption equilibrium capacity can be expressed as:

$$\frac{dq}{dt} = K_2(q_e - q_f)^2 \tag{4}$$

where K_2 is the rate constant of pseudo second-order sorption (g $mmol^{-1}$ min^{-1}). Integrating this equation and applying a boundary condition of $q = 0$ at $t = 0$ gives:

$$\frac{t}{q_t} = \frac{1}{K_2 q_e^2} + \frac{t}{q_e} \tag{5}$$

The sorption rate can be obtained from equation 6:

$$\frac{q_t}{t} = \frac{1}{(1/(K_2 q_e^2) + t/q_e)} \tag{6}$$

and the initial sorption rate, h, can be defined as

$$h = K_2 q_e^2 \tag{7}$$

Therefore, equation 8 can become

$$q_t = \frac{t}{\left((1/h) + (t/q_e)\right)} \tag{8}$$

The initial sorption rate, h (mmol g^{-1} min^{-1}), the equilibrium sorption capacity, q_e, and the pseudo second-order rate constant, K_2, can be determined experimentally from the slope and intercept of the plot of t/q_t *vs.* t.

Table 2. Kinetics parameters obtained for Ru adsorption onto clinoptilolite (pseudo first-order and pseudo second-order models).

	Pseudo first-order model			Pseudo second-order model		
$q_{e\ (exp.)}$ (mmol g^{-1})	k_1 (min^{-1})	$q_{e\ (theor.)}$ (mmol g^{-1})	R^2	K_2 (g $mmol^{-1}$ min^{-1})	q_e (mmol g^{-1})	R^2
0.164	0.021	0.111	0.9260	0.546	0.172	0.9998

The Elovich equation (Mclintock, 1967) is given as follows:

$$q_t = \frac{\ln(\alpha\beta)}{\beta} + \frac{\ln t}{\beta} \quad (9)$$

where q_t is the sorption capacity at time t, α is the initial sorption rate of the Elovich equation (mmol g^{-1} min^{-1}), and the parameter β is related to the extent of surface coverage and activation energy for chemisorption (g $mmol^{-1}$). The constants can be obtained from the slope and intercept of the linear relationship of q_t *vs.* ln t. The intra-particle diffusion model (Weber and Morris, 1963) is

$$q_t = K_{diff} t^{1/2} + C \quad (10)$$

where K_{diff} is the intra-particle diffusion rate constant (mmol g^{-1} $min^{-1/2}$) and C is the intercept.

Parameters and correlation coefficients for four kinetics models for Ru adsorption on the zeolite were calculated from corresponding plots (Tables 2 and 3). The value of R^2 for the pseudo second-order kinetics model was greater than for the other models. According to this rate law, the rate of sorption depends on the sorption capacity but not on the concentration of the sorbate. The pseudo second-order mechanism is also generally applicable for the sorption of small metal ions and with a short contact time to equilibrium. It was, therefore, selected as the best model to fit the experimental data and was used to determine the activation energy, E_a, which was evaluated from the slope of ln K_2 *vs.* $1/T$ using the Arrhenius equation (Figure 6), *viz.*

$$\ln K_2 = \ln A - \frac{E_a}{RT} \quad (11)$$

where K_2 and A are the rate constant and temperature-independent factor (g $mmol^{-1}$ min^{-1}), respectively; E_a, the activation energy of the reaction of adsorption (J mol^{-1}); R, the gas constant (8.314 J mol^{-1} K^{-1}); and T, the adsorption at absolute temperature (K).

In order to obtain thermodynamic parameters, the distribution coefficient, k_d (mL g^{-1}), was determined according to

$$k_d = \left(\frac{(C_i - C_f}{C_i}\right) \times V/W \quad (12)$$

where C_i and C_f are the initial and final concentrations of the Ru in solution, respectively; W, the weight of zeolite (g); and V, the volume of the solution (mL).

The thermodynamic state functions, *i.e.* ΔH^o and ΔS^o, were calculated (Table 4) from the slopes and intercepts of the linear variation of ln k_d with the reciprocal of the temperature, $1/T$ (Figure 7).

$$\ln k_d = -(\Delta H^o/RT) + (\Delta S^o/R) \quad (13)$$

The Gibbs free energy of adsorption, ΔG^o, was then calculated from:

$$\Delta G^o = \Delta H^o - T\Delta S^o \quad (14)$$

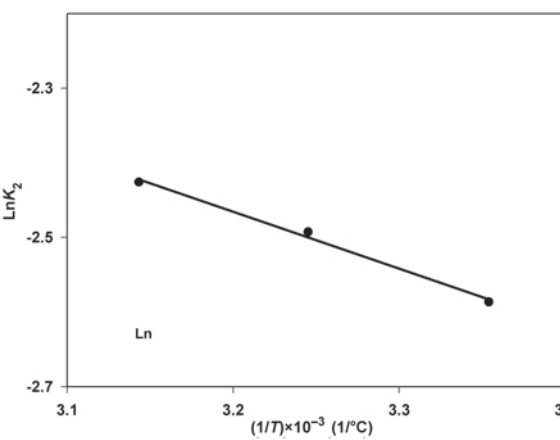

Figure 6. Linear least-squares method for calculating E_a.

Table 3. Kinetics parameters obtained for Ru adsorption onto clinoptilolite (Elovich and intra-particle diffusion models).

	Elovich model		Intra-particle diffusion model		
α (mmol g^{-1} min^{-1})	β (g $mmol^{-1}$)	R^2	k_{diff} (mmol g^{-1} $min^{-1/2}$)	C (mmol g^{-1})	R^2
0.0221	29.0	0.8206	0.0095	0.035	0.7424

Table 4. Activation energy (E_a) and thermodynamic parameters obtained for Ru adsorption onto natural clinoptilolite.

Temperature (ºC)	E_a (kJ mol^{-1})	ΔH^0 (kJ mol^{-1})	ΔS^0 (kJ mol^{-1} K^{-1})	ΔG^0 (kJ mol^{-1})
25	6.32	11.66	0.065	−7.71
35				−8.36
45				−9.01

The activation energy and enthalpy for the adsorption process were positive (Table 4). In other words, the adsorption of Ru species was an endothermic process. Endothermic adsorption means that higher temperatures favor adsorption of Ru (Figure 8) and a negative value for ΔG^o indicated that the adsorption process was favored.

Adsorption isotherms

Adsorption isotherms were plotted from the data obtained at different concentrations by means of the following equation (Figure 8):

$$a = [(C_i - C_e) \times V/m] \quad (15)$$

where a is the amount of metal species adsorbed by unit mass of zeolite (mg g^{-1}) at equilibrium; C_i and C_e are the initial and equilibrium concentration of Ru (mg mL^{-1}), respectively; m is the amount of zeolite (g); and V is the volume of Ru solution (mL). The value of a is valid for equilibrium at a particular temperature.

Two adsorption isotherm models were used to fit the experimental data. The Freundlich equation

$$a = K_F C^n \quad (16)$$

was initially applied in its linear form

$$\ln a = \ln K_F + n \ln C \quad (17)$$

where K_F is the known Freundlich constant related to the adsorbent capacity and n is an exponent related to the strength of the adsorption. The applicability of the Langmuir equation (equation 18) was also tested, where the constant K_L and the saturation capacity a_m were evaluated by regression analysis of its linear form (equation 19):

$$a = \frac{a_m K_L C}{(1 + K_L C)} \quad (18)$$

$$\frac{C}{a} = \frac{1}{a_m K_L} + \frac{1}{a_m} \times C \quad (19)$$

The correlation coefficients (R^2) of the linearized Langmuir and Freundlich adsorption isotherms (Figures 9 and 10) revealed better results from the Langmuir model (Table 5). The applicability of the Langmuir isotherm suggests monolayer coverage of the Ru species at the surface of the zeolite.

CONCLUSIONS

Local clinoptilolite was investigated as an adsorbent for Ru ions from aqueous solutions. The adsorption of Ru onto clinoptilolite was best described by the pseudo second-order rate model. The data also correlated well with the Langmuir adsorption model. Adsorption studies were also performed at different temperatures. The numerical value of ΔG^0 decreased with increasing temperature, indicating that adsorption was favored at

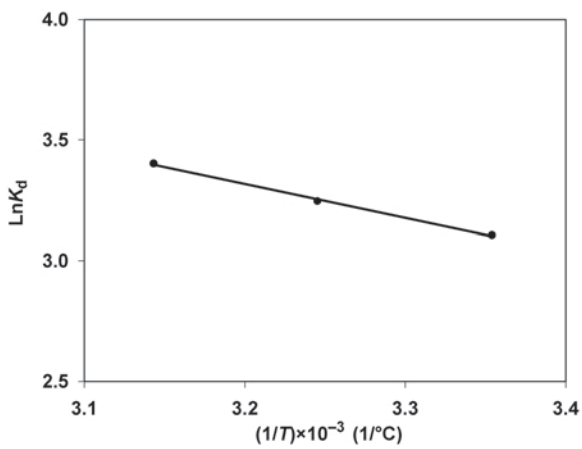

Figure 7. Linear least-squares method for calculating the thermodynamic parameters.

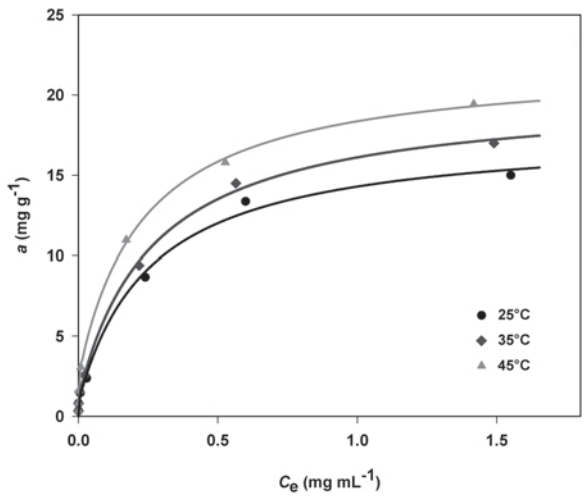

Figure 8. Adsorption isotherms at different temperatures.

Table 5. Adsorption isotherm parameters for Ru onto natural clinoptilolite.

Temp. (ºC)	Langmuir K_L (mL mg^{-1})	Langmuir a_m (mg g^{-1})	Langmuir R^2	Freundlich K_F (cm^3 g^{-1})	Freundlich n	Freundlich R^2
25	0.01165	15.60	0.9894	4.1973	0.4142	0.9798
35	0.01264	17.54	0.9878	3.7422	0.4304	0.9800
45	0.02004	19.61	0.9924	3.5467	0.4350	0.9776

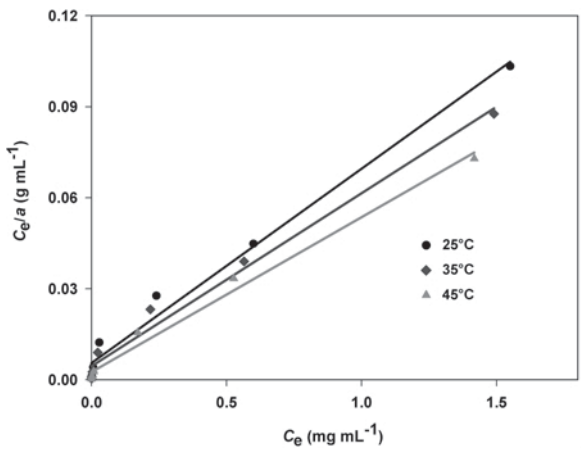

Figure 9. Linear least-squares method for calculating parameters of the Langmuir isotherm.

higher temperatures. The positive values of ΔH^0 revealed that the process was endothermic. These results will be helpful in the design of Ru-removal processes in the chemical industry using clinoptilolite as the adsorbent; clinoptilolite is also cheap and naturally abundant.

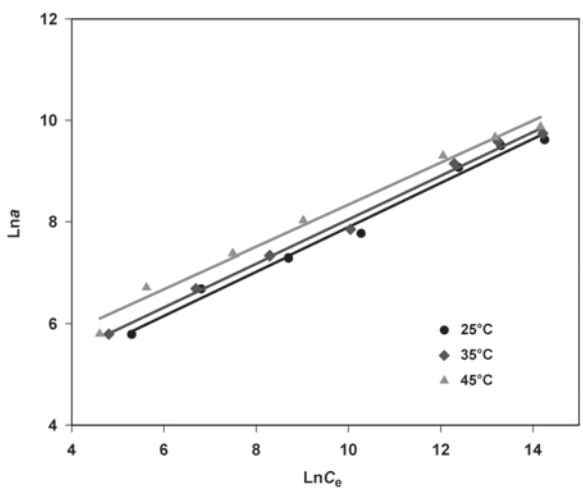

Figure 10. Linear least-squares method for calculating parameters of the Freundlich isotherm.

REFERENCES

Arambula-Villazana, V., Solache-Rios, M., and Olguin, M.T., (2006) Sorption of cadmium from aqueous solutions at different temperatures by Mexican HEU-type zeolite rich tuff. *Journal of Inclusion Phenomena and Macrocyclic Chemistry*, **55**, 237–245.

Avtokratova, T.D. (1963) *Analytical Chemistry of Ruthenium*. Israel Program of Scientific Translations, Jerusalem.

Balcerzak, M. (2002) Analytical methods for the determination of ruthenium: The state of the art. *Critical Reviews in Analytical Chemistry*, **32**, 181–226.

Barrer, R.M. (1985) *Hydrothermal Chemistry of Zeolites*. Academic Press, London.

Blanchard, G., Maunaye, M., and Martin, G. (1984) Removal of heavy metals from waters by means of natural zeolites. *Water Research*, **18**, 1501–1507.

Borai, E.H., Harjula, R., Malinen, L., and Paajanen, A. (2009) Efficient removal of cesium from low-level radioactive liquid waste using natural and impregnated zeolite minerals. *Journal of Hazardous Materials*, **172**, 416–422.

Breck, D.W. (1974) *Zeolite Molecular Sieves, Structure, Chemistry and Uses*. Wiley, New York.

Dyer, A. and Aggarwal, S. (1995) Removal of fission products from mixed solvents using zeolites. 1. Ruthenium removal. *Journal of Radioanalytical and Nuclear Chemistry*, **198**, 467–474.

El-Absy, M.A., El-Amir, M.A., Mostafa, M., Abdel Fattah, A.A., and Aly, H.M. (2005) Separation of fission produced ^{106}Ru and ^{137}Cs from aged uranium targets by sequential distillation and precipitation in nitrate media. *Journal of Radioanalytical and Nuclear Chemistry*, **266**, 295–305.

El-Naggar, M.R., El-Kamash, A.M., El-Dessouky, M.I., and Ghonaim, A.K. (2008) Two-step method for preparation of NaA-X zeolite blend from fly ash for removal of cesium ions. *Journal of Hazardous Materials*, **154**, 963–972.

Elizondo, N.V., Ballesteros, E., and Kharisov, B.I. (2000) Cleaning of liquid radioactive wastes using natural zeolites. *Applied Radiation and Isotopes*, **52**, 27–30.

Gandon, R., Boust, D., and Bedue, O. (1993) Ruthenium complexes originating from the PUREX process-coprecipitation with copper ferrocyanides via ruthenocyanide formation. *Radiochimica Acta*, **61**, 41–45.

Granados, F., Bertin, V., and Bulbulian, S. (2004) Speciation and adsorption of trace-level fission products of ^{132}Te, ^{95}Zr, ^{99}Mo and ^{103}Ru on inorganic materials. *Journal of Radioanalytical and Nuclear Chemistry*, **260**, 379–388.

Hong, S.H. and Grubbs, R.H. (2007) Efficient removal of ruthenium byproducts from olefin metathesis products by simple aqueous extraction. *Organic Letters*, **9**, 1955–1957.

Knight, D.W., Morgan, I.R., and Proctor, A.J. (2010) A simple oxidative procedure for the removal of ruthenium residues from metathesis reaction products. *Tetrahedron Letters*, **51**, 638–640.

Kokate, S.J. and Kuchekar, S.R. (2010) Reversed phase extraction chromatographic separation of ruthenium(III).

Journal of Saudi Chemical Society, **14**, 41–45.

Lopez, C.O., Perez, W.L., and Rodriguez, J. (2009) Ruthenium adsorption and diffusion on the GaN(0001) surface. *Applied Surface Science*, **255**, 3837–3842.

McLintock, I.S. (1967) The Elovich equation in chemisorption kinetics. *Nature*, **216**, 1204–1205.

Musić, S. and Ristic, M., (1987) Adsorption of microamounts of ruthenium on hydrous iron oxides. *Journal of Radioanalytical and Nuclear Chemistry*, **109**, 495–506.

Nassar, M.M., Ewida, K.T., Ebrahiem, E.E., Magdy, Y.H., and Mheaedi, M.H. (2004) Adsorption of iron and manganese ions using low-cost materials as adsorbents. *Adsorption Science & Technology*, **22**, 25–37.

Osmanlioglu, A.E. (2006) Treatment of radioactive liquid waste by sorption on natural zeolite in Turkey. *Journal of Hazardous Materials*, **137**, 332–335.

Qadeer, R. (2007) Adsorption behavior of ruthenium ions on activated charcoal from nitric acid medium. *Colloids and Surfaces A: Physicochemical and Engineering Aspects*, **293**, 217–223.

Rard, J.A. (1985) Chemistry and thermodynamics of ruthenium and some of its inorganic compounds and aqueous species. *Chemical Reviews*, **85**, 1–39.

Rathore, N.S., Pabby, A.K., and Venugopalan, A.K. (2004) Removal of actinides and fission products activity from intermediate alkaline waste using inorganic exchangers. *Journal of Radioanalytical and Nuclear Chemistry*, **262**, 543–549.

Schlesinger, R., Janietz, P., Heckner, K.H., and Rotsch, P. (1990) Radiochemical study of ruthenium adsorption from acid solution onto gallium arsenide surfaces. *The Journal of Physical Chemistry*, **94**, 8695–8702.

Schüth, F., Sing, K.S.W., and Weitkamp, J. (2002) *Handbook of Porous Solids*. Wiley-VCH, Weinheim, Germany.

Sharma, P., Singh, G., and Tomar, R. (2009) Synthesis and characterization of an analogue of heulandite: Sorption applications for thorium(IV), europium(III), samarium(II) and iron(III) recovery from aqueous waste. *Journal of Colloid and Interface Science*, **332**, 298–308.

Tanaka, H., Yamasaki, N., Muratani, M., and Hino, R. (2003) Structure and formation process of (K,Na)-clinoptilolite. *Materials Research Bulletin*, **38**, 713–722.

Taqui Khan, M.M., Ramachandraiah, G., and Rao, A.P. (1986) Ruthenium(III) chloride in aqueous solution: electrochemical and spectral studies. *Inorganic Chemistry*, **25**, 665–670.

Treacy, M.M.J. and Higgins, J.B. (2007) *Collection of Simulated XRD Powder Patterns for Zeolites*. Elsevier, Amsterdam.

Weber, W.J. and Morris, J.C. (1963) Kinetics of adsorption on carbon from solution. *Journal of the Sanitary Engineering Division*, **89**, 31–60.

Wilson, M.J., editor (1994) *Clay Mineralogy: Spectroscopic and Chemical Determinative Methods*. Chapman & Hall, New York.

(*Received 31 July 2010; revised 31 January 2011; Ms. 470; A.E. J.D. Fabris*)